Geochimica et Cosmochimica Acta xxx (xxxx) xxx

Contents lists available at ScienceDirect

Geochimica et Cosmochimica Acta

journal homepage: www.elsevier.com/locate/gca

Global cycling of vanadium isotopes from multiple ocean water masses and a restricted euxinic basin

Siqi Li [a,b,*], Sune G. Nielsen [c,d], Jeremy D. Owens [b]

[a] Department of Earth and Planetary Sciences, University of California, Riverside, Riverside, CA, USA
[b] Department of Earth, Ocean and Atmospheric Science, Florida State University and National High Magnetic Field Laboratory, Tallahassee, FL, USA
[c] Department of Geology and Geophysics, Woods Hole Oceanographic Institution, Woods Hole, MA, USA
[d] CRPG, CNRS, Université de Lorraine, 15 rue Notre Dame des Pauvres, 54501 Vandoeuvre lès Nancy, France

ARTICLE INFO

Associate editor: Thomas Johnson

Keywords:
Global seawater vanadium isotopic ($\delta^{51}V$) signatures
Black Sea seawater $\delta^{51}V$
Paleoredox proxy
Ancient marine redox evolution

ABSTRACT

To date, there have been only six vanadium isotope data ($\delta^{51}V$) points for open ocean seawater samples from four locations that lack vertical or spatial constraints. To provide more robust constraints on global seawater $\delta^{51}V$ signatures and explore the potential spatial deviations due to local/regional biogeochemical processes, we measured the V concentrations ([V]) and $\delta^{51}V$ values of seawater samples collected in the South Atlantic Ocean (GEOTRACES 40°S transect) and in the restricted euxinic Black Sea (MedBlack GEOTRACES cruises in 2013, R/V *Pelagia* cruise 64PE373; "euxinic" indicates free hydrogen sulfides in the water column). The South Atlantic sampling profiles intersect surface (~5 m) to bottom waters (~4500 m), which cover the major global ocean water masses that participate in large-scale ocean circulations. The two seawater samples in the Black Sea were collected at 100 and 150 m, across the anoxic-to-euxinic chemocline where dissolved V is proposed to be removed from the water column by sinking particulates. The results reveal relatively constant seawater V concentrations in deep water masses below the euphotic zone (>100 m) and a minor [V] depletion of ~6 % observed in the surface seawater samples (<100 m, within the euphotic zone) in the South Atlantic Ocean. The depletion is likely due to biological processes but is also modified by seawater mixing processes. The deep ocean water masses, except for the Antarctic Bottom Water, present relatively constant $\delta^{51}V$ values averaged at 0.27 ‰ ± 0.14 ‰ (2SD). In contrast, the Antarctic Bottom Water, which forms from the Antarctic continental margin, presents a relatively lighter seawater $\delta^{51}V$ value at 0.03 ‰, which may result from the local influence of the weathering inputs from the Antarctica continent but also requires further verification. Meanwhile, the surface seawater samples in the euphotic zone (<100 m) present heavier values averaged at 0.42 ‰ ± 0.08 ‰ (2SD) along with the minor depletion of seawater [V] relative to deeper water masses, which suggests a preferential uptake of ^{50}V during biological processes. The two Black Sea seawater samples show relatively low [V] values of around 16 nmol/kg in the shallow water columns and lighter seawater $\delta^{51}V$ values at 0.17 ‰ and −0.07 ‰, which should reflect a combination of the regional hydrological cycle and biogeochemical processes. This work now confirms the conservative nature of V isotopes in large-scale deep ocean circulations and provides a more robust framework for interpreting the marine sedimentary $\delta^{51}V$ variations. Furthermore, the distinguishable deviations of seawater $\delta^{51}V$ values due to the biological processes in the euphotic zone or weathering inputs in severely restricted basins analogous to the Black Sea and/or in near-coast environments also propose careful interpretation of ancient marine sedimentary $\delta^{51}V$ values that were documented under similar depositional environments.

1. Introduction

Marine redox conditions play an important role in the complex and critical surficial processes that have shaped the surface of the Earth in the past hundreds of millions of years. These include atmospheric oxygenation mediated by the burial of organics and sulfides under reducing marine conditions, the nutrient availability of bio-critical elements (e.g., sulfur (S), iron (Fe), phosphorus (P), and molybdenum

* Corresponding author at: Department of Earth and Planetary Sciences, University of California, Riverside, Riverside, CA, USA.
E-mail address: siqil@ucr.edu (S. Li).

https://doi.org/10.1016/j.gca.2025.08.037
Received 17 October 2024; Accepted 23 August 2025
Available online 25 August 2025

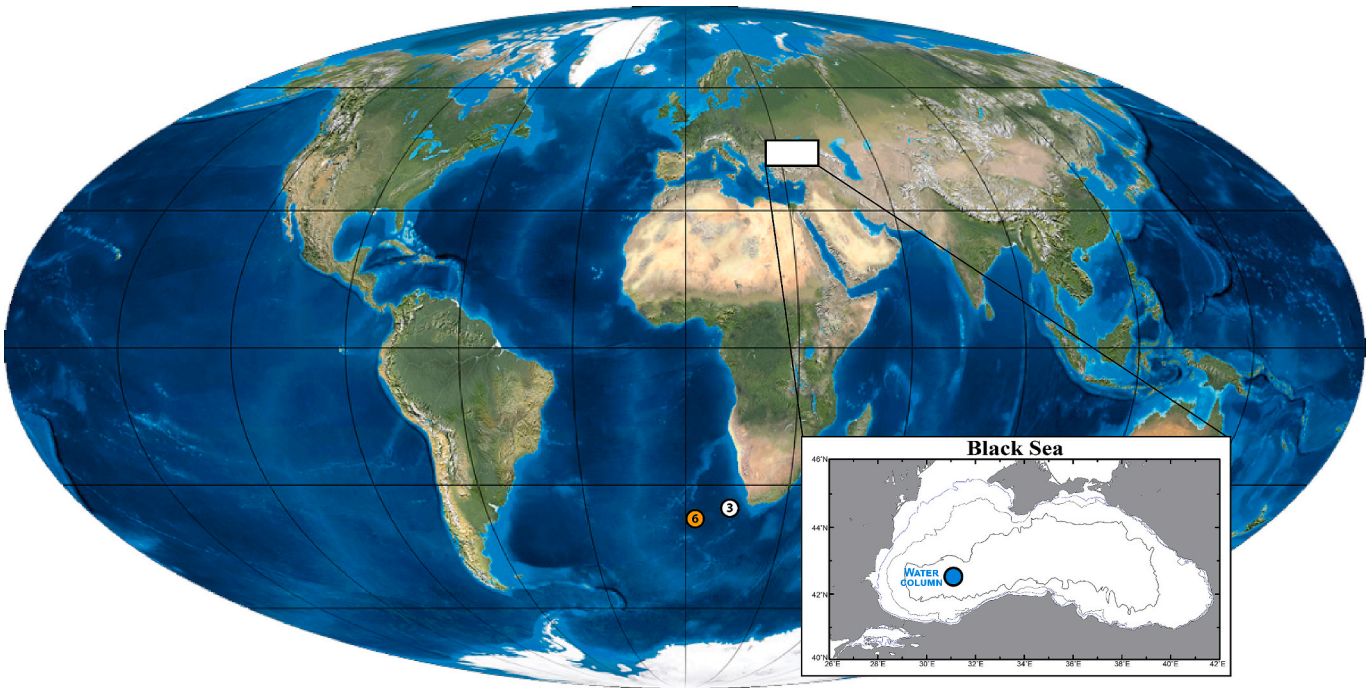

Fig. 1. The locations of Station 3 (white spot) and Station 6 (orange spot) at ~ 40°S in the South Atlantic Ocean and the studied location in the Black Sea (blue spot). The map is modified from Owens et al. (2017).

(Mo)), and marine ecological and biological evolutionary trajectories (e.g., ancient marine biodiversification and mass extinction events; Berner, 2013; Evans et al., 2018; Lindskog et al., 2023; Lyons et al., 2014; Moore et al., 2017; Owens et al., 2016; Reinhard et al., 2020; Robbins et al., 2016; Sperling et al., 2022). However, certain aspects of Earth's redox history remain debated, especially due to the difficulty in distinguishing low levels of marine oxygenation. For instance, the Ediacaran metazoan radiation might have required low dissolved oxygen levels that were similar to those of modern oxygen minimum zones (Cole et al., 2020). However, such low-oxygen conditions cannot readily be constrained using current widely utilized geochemical tools, such as Fe speciation and Mo, uranium (U), and thallium (Tl) isotopes. As a result, discordance between the fossil evidence and the geochemical proxies can occur (Li et al., 2023). Refined constraints on such low-oxygen conditions may help disentangle the influence of marine deoxygenation from other environmental drivers such as sea level and ocean pH changes.

The V isotope composition documented in sediments has been proposed as a proxy for changes in marine oxygenation, with a particular potential to distinguish low-oxygen-to-anoxic transitions with an $[O_2]$ threshold at ~ 10 μM (Wu et al., 2020). The dissolved V in modern open oceans is dominated by pentavalent vanadate species (valence state: V^{5+}), $H_2VO_4^-$ and HVO_4^{2-}, with a concentration range of around 35 nM and a residence time of ~ 90 kyr (thousand years; Nielsen, 2020). The relatively short residence time compared with U (400–500 kyr, Zhang et al., 2020) and Mo (~440 kyr, Kendall et al., 2017), but much longer than the global ocean circulation (~2 kyr), suggests a more rapid response to changes in ocean oxygenation, in particular those operating close to anoxic conditions. The mass balance of V isotopes in the modern oxic oceans presumes a globally homogeneous seawater $\delta^{51}V$ value. This has been utilized to track ancient marine redox fluctuations, both in the spatial expansion and the severity of oxygen depletion (Heard et al., 2023; Li et al., 2023; Nielsen, 2020; Wei et al., 2023). However, the limited seawater $\delta^{51}V$ datasets for global seawater $\delta^{51}V$ signatures, consisting only of six discrete samples from four locations in the East Pacific Ocean, the North Atlantic Ocean, and the Gulf of Mexico (Wu et al., 2019), still render the assertion of global homogeneous seawater $\delta^{51}V$ values uncertain. In particular, it is possible that local/regional impacts such as the biological uptake of V in shallow seawater and the riverine inputs in coastal areas and/or severely restricted basins could cause departures from otherwise conservative V isotope behavior (Collier, 1984; Ho et al., 2018; Schuth et al., 2019).

Here we present new seawater [V] and $\delta^{51}V$ profiles from samples collected during GEOTRACES at the ~ 40°S South Atlantic Ocean transect (Mawji et al., 2015). The sampling depths span from 5 to 4,500 m, where the sampling profiles intersect nearly all major global water masses including the Antarctic Bottom Water (AABW). We also measured the [V] and $\delta^{51}V$ values of two seawater samples collected at 100 and 150 m in the Black Sea during the MedBlack GEOTRACES cruises in 2013 (R/V *Pelagia* cruise 64PE373) across the anoxic-to-euxinic chemocline ("euxinic" indicates free hydrogen sulfides in the water column) in the shallow water column. The Black Sea is subject to the basinal mixing processes of surrounding riverine inputs and seawater inputs from the Mediterranean Sea through the Bosporus Strait. Therefore, this work provides more systematic constraints on global seawater $\delta^{51}V$ homogeneity and potential spatial deviations due to local or regional processes, which are critical for more explicit interpretations of ancient sedimentary $\delta^{51}V$ records.

2. The hydrological background of the studied locations

2.1. The 40°S South Atlantic Ocean

The seawater samples were collected at Station 3 (36.46°S, 13.39°E) and Station 6 (39.99°S, 0.92°E) off the South African coast during the UK GEOTRACES cruise GA10/D357 Leg 1 (Fig. 1). The collection protocols of seawater samples were described in detail in previous work, and seawater samples were acidified to pH ~ 2 with trace-metal clean HCl for long-term storage (Horner et al., 2015; Owens et al., 2017).

The water column transect across the Atlantic Ocean at ~ 40°S intersects water masses sourced from different ocean basins (Wyatt et al., 2014). Surface seawater is influenced by the warm and salty southward-flowing Sub-Tropical Surface Water and the cold and fresh northward-flowing Sub-Antarctic Surface Water, with intrusion from the leakage of the warm and saline Agulhas Current from the Indian Ocean between

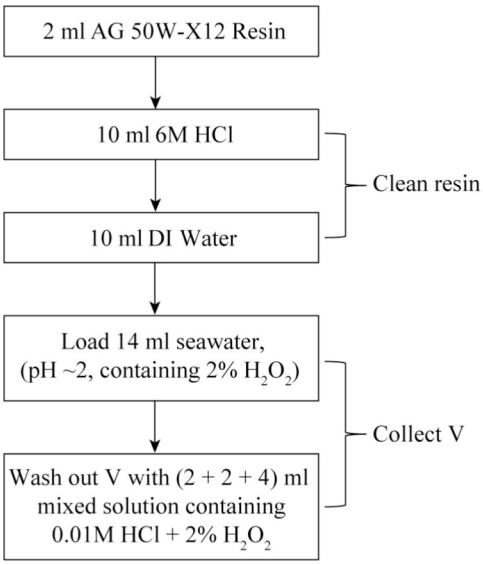

Fig. 2. The column chromatography procedures to preconcentrate V for seawater [V] measurement. Vanadium is collected with the 2 % H_2O_2-containing solution as pervanadyl cations (VO_2^+) under acidic conditions (pH < 2) are transformed to peroxovanadate anions that are disassociated from the cation resin.

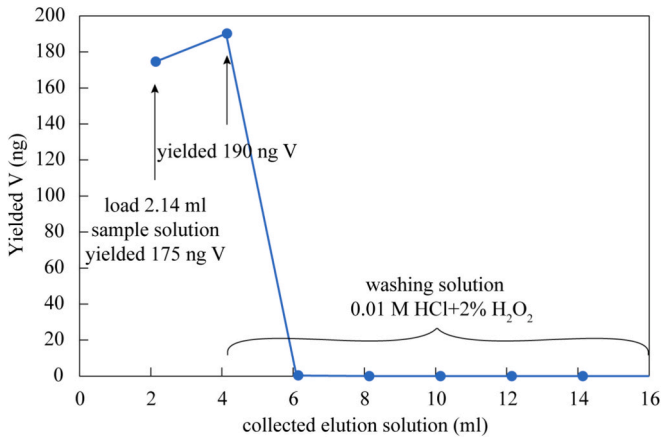

Fig. 3. The V elution curve of the column chromatography method as illustrated in Fig. 2. The method was tested with 2.14 ml artificial seawater containing 2 % H_2O_2 (2 ml artificial seawater doped with 365 ng V + 140 µl 30 % H_2O_2). The result shows that V is quantitatively yielded from the resin column.

10°E and South Africa (Conway et al., 2016; Lutjeharms, 2006; Paul et al., 2015). The Antarctic Intermediate Water (AAIW), forming at the Antarctic Convergence zone, presents cold and less saline seawater (with a salinity minimum $S < 34.4$) and is located at a depth of around 500 to 1250 m. The Upper Circumpolar Deep Water (UCDW) originates from the deep water of the Pacific and Indian Oceans and spans a depth of around 1250 to 1,750 m. The underlying southward-flowing North Atlantic Deep Water (NADW) presents a salinity maximum ($S > 34.7$) in deep waters and occupies a depth between around 1750 and 4000 m in the Cape Basin. The coldest and densest Antarctic Bottom Water (AABW), forming in the Antarctic continental shelf regions (Gordon, 2001; Solodoch et al., 2022), resides at a depth >~4000 m.

The samples analyzed in this work include depths from surface seawater to ~ 4500 m——the first study to do so. Thus, all major water masses in the South Atlantic are represented within our sample set and should allow an assessment of potential variation in $\delta^{51}V$ for the major global water masses.

2.2. The Black Sea

The Black Sea is a restricted basin receiving freshwater inputs into the upper oxic water column from surrounding rivers and seawater fluxes mainly from the Mediterranean Sea through the Bosporus Strait, with the seawater plume exiting the strait below a depth of around 50 m and sinking along the continental shelf and slope (Kara et al., 2008; Stanev et al., 2001). The shallow and strong pycnocline causes strong stratification, and hence restrains vertical mixing and leads to slow renewal of the bottom water. The basin-scale circulation is mainly driven by winds and the dense Mediterranean seawater plume from the Bosporus Strait (Stanev, 2005). The strong stratification and slow basinal mixing results in permanent euxinic deepwater, which has been in place since the mid to late Holocene (Arthur and Dean, 1998; Eckert et al., 2013).

The Black Sea seawater samples analyzed here were collected at Station 2 during Leg 2 of the MedBlack GEOTRACES cruises in 2013 (64PE373, R/V *Pelagia*; Fig. 1). The seawater samples were filtered and acidified to pH ~ 2 with ultrapure HCl for long-term storage (Owens et al., 2017; GA04N Section (leg 2), n.d.). The dissolved [O_2] in the water column decreased from ~ 200 µmol/kg at a depth of 50 m to nearly zero at a depth of ~ 100 m, followed by the initiation of euxinic conditions (Vance et al., 2016). The two seawater samples measured in this work were collected at depths of 100 and 150 m, respectively, across the anoxic-to-euxinic chemocline zone.

3. Methods

3.1. Measurement of seawater [V]

It is difficult to measure the seawater V concentration precisely through direct dilution due to high salinity and low V concentrations. Therefore, we utilized the BIO-RAD AG 50W-X12 cation resin to remove matrix elements and preconcentrate V before measurement (similarly to the methods utilized in Nielsen et al., 2011; Wu et al., 2016). All the chemical reagents utilized in this work were trace-metal-clean, and the cation and anion resins were cleaned alternately with 6 M HCl and deionized (DI) water before application. A column chromatography method utilizing the pre-cleaned BIO-RAD Poly-Prep chromatography column (9 cm high and 2 ml bed volume) loaded with 2 ml BIO-RAD AG 50 W-X12 cation resin was established (Fig. 2). The cation exchange capacity of AG 50 W-X12 is ~ 2.1 meq/ml (referred to AG 50 W and AG MP-50 Cation Exchange Resins Instruction Manual, BIO-RAD). The mechanism is to sequester major matrix elements (e.g., Na, Mg, Ca, and K) onto the cation resin under weakly acidic conditions (pH at ~ 2) and yield V by transforming pervanadyl cations to peroxovanadate anions with H_2O_2 solution (Andersson et al., 2000). This method was first tested with 2 ml artificial seawater (acidified to pH at ~ 2) doped with 365 ng V to check if V could be disassociated efficiently from the cation resin and recovered quantitatively with the weakly acidic diluted H_2O_2 solution (WAD H_2O_2 containing 0.01 M HCl + 2 % H_2O_2). Around 140 µl 30 % H_2O_2 (BDH Aristar Ultra) was added to the 2 ml artificial seawater, right before loading into the 2 ml chromatography column, to obtain 2 % H_2O_2. After the complete dripping of the sample solution, the WAD H_2O_2 solution was loaded into the column with 2 ml each time pending the complete dripping of the previous solution. All the elution cuts were collected with 7-ml Teflon beakers and dried on a hot plate. After that, 0.5 ml 15 M HNO_3 and 0.5 ml 30 % H_2O_2 were added to each beaker to digest remnant organic matter under 120 °C on the hot plate. Then the solution was completely dried to remove chloride, as molecular species such as $^{35}Cl^{16}O$ and $^{37}Cl^{14}N$ can interfere with ^{51}V signal. The solid was redissolved in 2 ml 2 % HNO_3 for the following instrumental measurement. The yielded V was measured with Agilent 7500ce ICP-MS at the National High Magnetic Field Laboratory (NHMFL), with indium doped to monitor the instrumental stability. Two artificial in-lab vanadium

Table 1
The measured [V] values of the seawater standard NASS-6.

Seawater Standard	$[V]_{measured}$ ng/g	$[V]_{average}$ ng/g	$[V]_{certified}$ ng/g[a]
NASS-6-rep1(1)	1.25	1.26 ± 0.02 (1SD)	1.42 ± 0.16
NASS-6-rep1(2)	1.29		
NASS-6-rep2(1)	1.26		
NASS-6-rep2(2)	1.25		

Notes: The "rep" indicates that the seawater aliquots were reprocessed with the column chromatography method for remeasurement. The number in the bracket indicates the duplicate measurement of the same sample solution with Thermo ELEMENT 2 ICP-MS.
[a] The certified [V] value of the NASS-6 seawater reference material is from the National Research Council of Canada.

solutions with concentrations of 20 and 40 ppb diluted from Alfa Aesar vanadium (AA-V) standard solution (Nielsen et al., 2011) were utilized to monitor instrumental accuracy. The instrumental precision (1RSD) is better than 5 %. The elution curve (Fig. 3) shows that V is quantitatively recovered with a 100 % yield rate. To measure seawater [V], around 14 ml seawater sample (to yield around 25 ng V for concentration measurement) was doped with 30 % H_2O_2 and then loaded onto the resin column and processed with procedures illustrated in Fig. 2. As the total cation exchange capacity of the 2-ml resin column is around 4.2 meq/ml, whereas 14 ml seawater contains a cation equivalent of ~ 8.5 meq, the left salts were redissolved in 5 ml WAD H_2O_2 solution and reprocessed with this column chromatography method. Finally, the collected solution was dried and then digested with the mixed HNO_3 and H_2O_2 solution as aforementioned. For each seawater sample, at least 80 % of the total matrix salts can be removed after the duplicate column method, as estimated with the remnant solid mass (less than ~ 80 mg) compared with the original salt content (~490 mg). The aliquots of seawater standard NASS-6 from the National Research Council of Canada as reference materials and the blank column (no sample solution loaded) for background monitoring were also processed in parallel with the same chemical procedures. The V concentrations were measured with a Thermo Element 2 ICP–MS using medium resolution at NHMFL. Indium was utilized as an internal standard to monitor long-term instrument stability. The background V in the column blank was lower than the detection limit. The average value of measured NASS–6 seawater [V] is 1.26 ± 0.02 ng/g, slightly lower than the certified value reported by National Research Council of Canada (see Table 1). The seawater samples are presented in Table 2. For samples with duplicate measurements (as denoted with "dup" in Table 2), the uncertainty 1RSD is calculated; otherwise an instrumental measurement precision with 1RSD better than 5 % is assigned.

Table 2
The seawater salinity, [V], and $\delta^{51}V$ values at Station 3 and Station 6 in the South Atlantic Ocean and in the upper water columns in the Black Sea.

Sample ID	Depth m	Salinity psu	Seawater [V] ng/g	Seawater [V] nmol/kg[a]	1RSD %	Seawater [V] nmol/kg[b]	Yielded [V] ng/g	Yielding rate %	$\delta^{51}V$ ‰	2SD ‰	N
Station 3											
00-186	5	34.88	1.80	34.8	2.6	34.9	1.47	83	0.43	0.05	3
00-186-dup	5	34.88	1.74								
00-184	23	34.88	1.76	34.1	2.3	34.2	1.34	77	0.38	0.11	3
00-184-dup	23	34.88	1.71								
00-181	42	34.88	1.76	33.9	2.6	34.0	1.46	85	0.42	0.06	2
00-181-dup	42	34.88	1.69								
00-178	97	34.74	1.73	34.0	5.0	34.3	1.40	81	0.32	0.07	3
00-169	989	34.41	1.80	35.3	5.0	35.9	N/A	N/A	0.36	0.03	4
00-168	1483	N/A	1.80	35.4	5.0	N/A	N/A	N/A	0.32	0.05	2
00-166	2955	N/A	1.71	33.7	5.0	N/A	N/A	N/A	0.14	0.02	2
00-164	3931	34.75	N/A	N/A		N/A	N/A	N/A	0.24	0.08	2
Station 6											
0-451	5	34.54	1.65	32.8	1.1	33.2	1.41	85	0.49	0.10	4
0-451-dup (1)	5	34.54	1.69								
0-451-dup (2)	5	34.54	1.67								
0-449	23	34.54	1.70	33.7	0.8	34.1	1.38	80	0.44	0.09	3
0-449-dup	23	34.54	1.72								
0-446	47	34.54	1.68	32.9	0.5	33.4	1.55	92	0.38	0.16	2
0-446-dup	47	34.54	1.67								
0-443	98	34.54	1.80	34.7	2.2	35.2	1.57	89	0.43	0.09	5
0-443-dup	98	34.54	1.74								
0-433	1498	34.61	1.85	36.4	5.0	36.8	N/A	N/A	0.31	0.02	2
0-432	1999	34.77	1.83	36.0	5.0	36.2	1.29	71	0.24	0.08	2
0-431	2998	34.83	1.78	34.9	5.0	35.1	1.41	79	N/A		
0-429	4000	34.75	1.82	35.6	5.0	35.9	1.50	83	0.24	0.04	2
0-428	4501	34.73	1.81	35.4	5.0	35.7	1.67	92	0.03	0.03	3

Sample ID	Depth m	Salinity ‰	Seawater [V] ng/g	Seawater [V] nmol/kg[a]	1RSD %	Seawater [V] nmol/kg[b]	Yielded [V] ng/g	Yielding rate %	$\delta^{51}V$ ‰	2SD ‰	N
Black Sea											
BS 100	100	N/A	0.818	16.1	5.0	N/A	0.61	75	0.17		1
BS 150	150	N/A	0.777	15.2	0.6	N/A	0.56	72	−0.07		1
BS 150-dup	150		0.771								

Artificial seawater standard	V doped ng	Yielded [V] ng	Yielding rate %	$\delta^{51}V$ ‰	2SD ‰	N
SW Matrix-AA	910	797	88	0.04		1
SW Matrix-BDH	900	N/A	N/A	−1.09	0.11	2

Notes: The salinity data are from Conway et al. (2016) and Horner et al. (2015). The "dup" and the number in the bracket indicate the re-dilution and remeasurement of the same solution.
[a] The seawater V concentration is averaged with duplicate measurements. The uncertainty 1RSD is calculated with duplicate measurements, otherwise the instrumental measurement precision with 1RSD better than 5% is assigned. For samples with duplicate measurements, the average values are adopted in text and figures.
[b] The seawater V concentration is normalized to salinity 35‰.

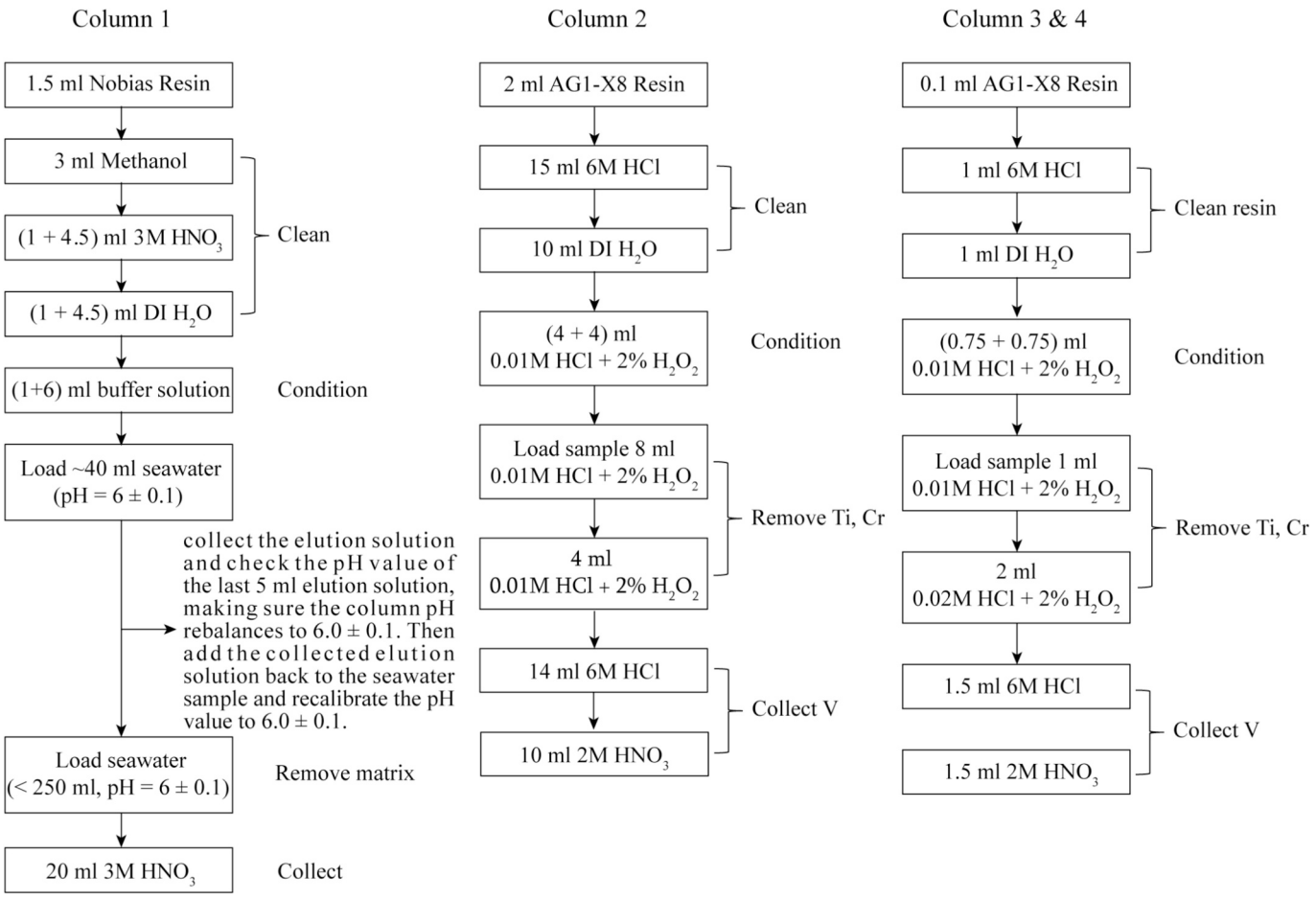

Fig. 4. The column chromatography procedures modified from Wu et al. (2019) to preconcentrate and purify V from seawater samples for isotopic measurement. The first and second columns are modified to reduce V loss and the third and fourth columns are similar to the original method (Wu et al., 2019), since no V loss was observed as the two steps were processed in this work.

3.2. *Measurement of seawater $\delta^{51}V$*

To separate V from the seawater matrix for isotope ratio measurements, we adopted the four-column chromatography method established by Wu et al. (2019) utilizing the Hitachi Nobias Chelate PA-1 resin and the AG1-X8 anion resin (BIO-RAD). This method exploits the pH-dependent adsorption of V onto Hitachi Nobias Chelate PA-1 resin, and an optimal operating pH range of 6.0 ± 0.1 is adopted to preconcentrate V from seawater samples (Wu et al., 2019).

However, as seawater was loaded into the pre-cleaned and −conditioned PA-1 resin column, we noticed a pH shift of the elution solution from inceptive 6 ± 0.1 to ~ 5, which likely indicates a release of H^+ from the resin caused by ion exchange between the seawater and the resin. The pH value of the elution solution would gradually shift back to ~ 6 after about 40 ml of seawater had been eluted. This pH shift may partially account for the significant loss of V in previous research (Wu et al., 2019), considering that a total volume of ~ 250 ml of seawater was loaded into each column (Wu et al., 2019). Furthermore, for the second column utilizing 2 ml AG1-X8 anion resin (BIO-RAD) to remove the remnant matrix elements and Cr and Ti, as described in Fig. 1b in Wu et al. (2019), we also observed occasional V loss that could exceed 100 ng, as in the elution solution (collected from the loaded sample solution and the following 15 ml cleaning solution), before V collection. This loss of V may also cause relatively low yields, considering that 500 ml seawater contains only around 900 ng V and a loss of ~ 100 ng would be about 10 %. No significant V loss was observed for the third and fourth mini columns (Wu et al., 2019). Therefore, to improve the seawater V yield, we modified the chemical procedures for the first and second columns, which are illustrated in Fig. 4. For the first column, utilizing Nobias resin, as the seawater sample is loaded into the column, the elution cuts are collected to monitor pH shift until the pH value returns to 6.0 ± 0.1 (around 40 ml seawater is consumed at this step). Then the collected elution solution is combined with the remaining seawater sample and the pH value recalibrated to 6.0 ± 0.1 with acetic acid (BDH Aristar Ultra) and ammonia solution (Suprapur). After that, the seawater sample is reloaded into the column and V collected with 3 M HNO_3 (Fig. 4). For the second column, the cleaning solution is decreased from 15 ml (see Fig. 1b in Wu et al., 2019) to 4 ml to reduce potential V loss. Alternatively, the cation column chromatography method for the seawater V concentration measurement, as illustrated in Fig. 2, might substitute for the second column in Fig. 4 to eliminate the remnant matrix and avoid potential V loss, although this has not been tested yet. The matrix solutions of two seawater samples were collected after the first column chemistry and were separately doped with ~ 900 ng AA-V (SW Matrix-AA) and ~ 900 ng BDH–V (SW Matrix-BDH). The two synthetic standards were re-buffered to ensure a pH value of 6.0 ± 0.1 and were processed with the column chemistry (Fig. 4). After the column chromatography, samples were dried on a hot plate at ~ 120℃ and then heated further at ~ 200℃ for several hours to drive off the remanent sulfur (Nielsen et al., 2016). Before the isotopic analysis, the yielded V of seawater samples and synthetic standards were measured in the same measurement sequence for seawater V concentration with the Thermo Element 2 ICP–MS, following the same protocols (see *Measurement of seawater [V]*). The background V blank was monitored through regular blank checks for pre-cleaned containers, buffer solutions, and collected cleaning solutions through columns before loading samples. The average

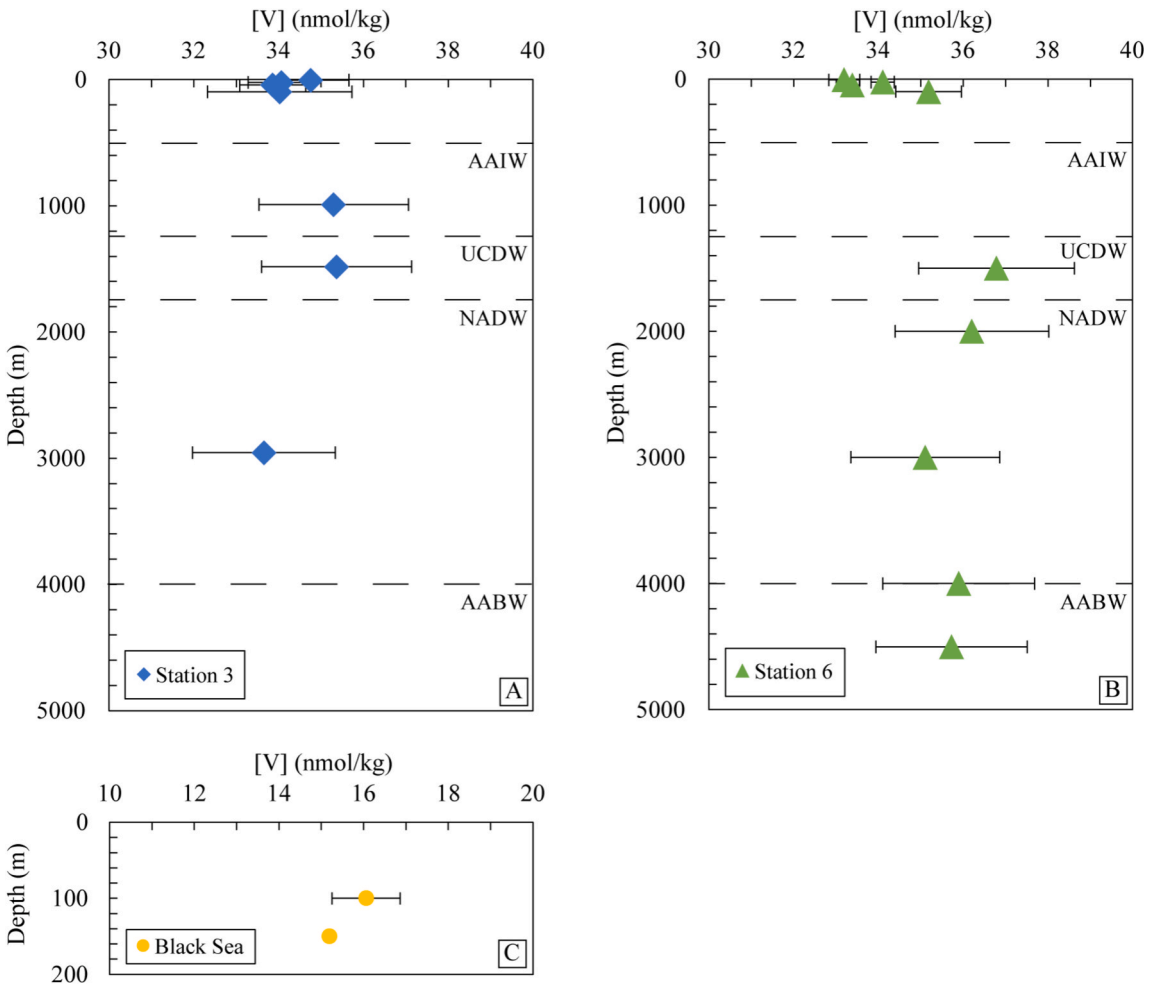

Fig. 5. The seawater [V] values at Station 3 (panel A) and Station 6 (panel B) in the South Atlantic Ocean, and in the upper water columns in the Black Sea (panel C). The seawater transects in the South Atlantic Ocean: Antarctic Intermediate Water (AAIW), Upper Circumpolar Deep Water (UCDW), North Atlantic Deep Water (NADW), and Antarctic Bottom Water (AABW).

V background value during the chemical procedures is around 4 ng for each seawater sample. The modified column chromatography method (Fig. 4) for seawater V isotopic measurement also presents significantly improved V yield rates at around 80 to 90 % for most of the Atlantic seawater samples, though the two seawater samples from the Black Sea still present lower yields at ~ 70 %, which is probably attributed to the lower total loaded amount of V (~800 ng in 1000 ml seawater; Table 2).

The V isotopic compositions were measured with the standard (AA-V)-sample bracket method with a Neptune Multi-collector-ICP-MS at the NHMFL. The Faraday cups were set following configurations described in Nielsen et al. (2016), except that the 10^{11} Ω resistor was applied to monitor the ^{50}V signal. The BDH-V standard solution was utilized to monitor the long-term in-lab instrumental precision (2SD at 0.11 ‰) and accuracy (Li et al., 2023). The artificial seawater standards, SW Matrix-AA and SW Matrix-BDH, present a value of 0.04 ‰ ($N = 1$) and −1.09 ‰ ± 0.11 ‰ (2SD, $N = 2$), respectively, in good agreement with values of the pure V standards AA–V (0 ‰, Nielsen et al., 2011) and BDH–V (−1.19 ‰ ± 0.12 ‰, Nielsen et al., 2011; −1.23 ‰ ± 0.08 ‰, Wu et al., 2016; −1.19 ‰ ± 0.15 ‰, Wu et al., 2019; −1.18 ‰ ± 0.11 ‰, Li et al., 2023). This also demonstrates the nearly complete extraction of V from the natural seawater samples after the first column and limited systematic isotopic fractionations that cannot be identified with current analytical precision during the column chromatography chemistry. The 2SD for the Black Sea seawater samples cannot be calculated directly due to limited seawater volume. Here we assign the worst 2SD value of 0.16 ‰ of our isotope measurement, although most seawater samples have uncertainties better than the long-term in-lab instrumental precision.

4. Results

The seawater [V] and $\delta^{51}V$ values are presented in Table 2. Station 3 displays a relatively invariant seawater [V] profile with the seawater [V] values varying between 33.7 and 35.4 nmol/kg, averaged at 34.4 nmol/kg (Fig. 5A). The shallow euphotic zone seawater exhibits an average value of 34.2 ± 0.47 (1SD) nmol/kg, compared with an average value of 34.6 ± 0.87 (1SD) nmol/kg for deep seawater [V]. The difference in seawater [V] from the euphotic (eu) zone and deep seawater, as estimated with average (ave) values and error propagation, $\frac{[V]_{ave\_deep}-[V]_{ave\_eu}}{[V]_{ave\_deep}}$, is 1.2 % ± 2.9 % (1SD), indistinguishable from the uncertainty. In contrast, Station 6 presents a slightly more variable seawater [V] profile between 32.8 and 36.4 nmol/kg (Fig. 5B). The shallow euphotic zone seawater exhibits an average value of 33.5 ± 0.89 (1SD) nmol/kg, compared with an average value of 35.7 ± 0.54 (1SD) nmol/kg for deep seawater [V]. The difference in seawater [V] from the euphotic zone and deep seawater is 6.2 % ± 2.9 % (1SD), indicating minor depletion in euphotic seawater [V]. Regardless of the slightly different surface seawater [V] values, the two stations display similar seawater $\delta^{51}V$ profiles with heavier values between 0.3 ‰ and 0.5 ‰ (averaged at 0.42 ‰ ± 0.08 ‰, 2SD) in the euphotic seawater samples, which are significantly different from the generally consistent $\delta^{51}V$ values in deep water

Table 3
The *t*-test (assuming unequal variances, significance level at 0.01) for the seawater $\delta^{51}V$ signatures of the surface seawater (<100 m, Variable 1) and the deep water (>100 m, Variable 2) at ~ 40°S in the South Atlantic Ocean.

	Variable 1	Variable 2
Mean	0.424	0.271
Variance	0.001	0.005
Observations	7	8
Hypothesized mean difference	0	
df	11	
t Stat	5.356	
$P(T \leq t)$ two-tail	0.000232	
t critical two-tail	3.106	

Note: The AABW is not included due to local influence.

masses at around 0.2 ‰ to 0.3 ‰ (averaged at 0.27 ‰ ± 0.14 ‰, 2SD; Table 3), although a relatively lower value of 0.03 ‰ was observed in AABW (Fig. 6A and 6B).

The two Black Sea seawater samples contain similar and relatively low V concentrations at 16.1 and 15.2 nmol/kg (Fig. 5C). Their $\delta^{51}V$ values of 0.17 ‰ and −0.07 ‰ are lower than for the open oceans (Fig. 6C).

5. Discussion

5.1. The seawater [V] and $\delta^{51}V$ profiles at ~ 40°S in the South Atlantic Ocean

The seawater [V] values measured at ~ 40°S in the South Atlantic Ocean vary between 32.8 and 36.4 nmol/kg. These results are similar to previously reported seawater [V] values in the Pacific and Atlantic Oceans (Collier, 1984; Ho et al., 2018; Mlddelburg et al., 1988; Sherrell and Boyle, 1988), and imply relatively conservative seawater V behavior in open oceans. At Station 6, the euphotic zone displays a minor depletion of seawater [V] and heavier $\delta^{51}V$ signatures than in deep seawater masses (Fig. 7). This V depletion coincides with the severe depletion of macronutrients (phosphate and nitrate) in the euphotic zone (Archer et al., 2020; Horner et al., 2015), suggesting a correlation that may indicate biological uptake of V. However, a similar correlation between [V] depletion and positive $\delta^{51}V$ shift is not observed at Station 3 (Fig. 7), even though severe consumption of macronutrients is also observed (Archer et al., 2020). On the other hand, the shallow seawater at ~ 40°S between South Africa and 10°E may be due to an impact or a signal from the Agulhas Current, which comes from the Indian Ocean and is characterized by warmer temperatures and higher salinity and nutrients (Conway et al., 2016; Lutjeharms, 2006; Paul et al., 2015). Such mixing processes thus may obscure the minor seawater [V] depletion in the euphotic zone relative to deeper water masses at Station 3, while macronutrients are efficiently ingested by phytoplankton. Although the seawater mixing makes it difficult to quantify the biological uptake of V precisely, especially for these localities, we here utilized a simple mass balance calculation that predicts the V isotope compositions carried in biota ($\delta^{51}V_{bio}$) as a function of the fraction (i.e., the proportion, *f*) of V removed by biota:

$$\delta^{51}V_{bio} = \delta^{51}V_{ini} + \left(1 - \frac{1}{f}\right) \cdot \Delta^{51}V_{shift}. \quad (1)$$

The initial seawater $\delta^{51}V$ value ($\delta^{51}V_{ini} = 0.2$ ‰) is based on the average deepwater V isotope value (this study; Wu et al., 2019), whereas the positive isotopic shift of seawater $\delta^{51}V$ value ($\Delta^{51}V_{shift} = 0.1$ to 0.2 ‰) occurs due to the biological uptake. The result shows that the biota preferentially takes up ^{50}V, and the $\delta^{51}V$ signatures of biota can be as negative as −1.4 to −2.9 ‰ for a 6 % depletion of seawater [V], as shown at Station 6 (Fig. 8), indicating pronounced V isotopic fractionation during potential biological uptake. Chételat et al. (2021)

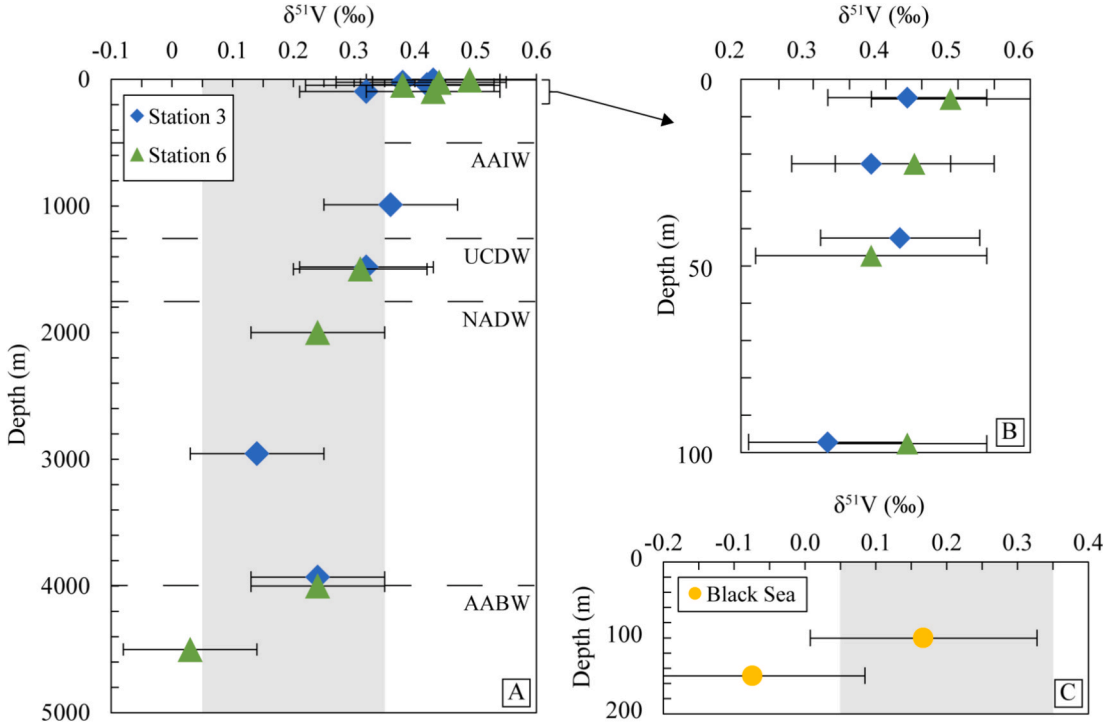

Fig. 6. The seawater $\delta^{51}V$ values at Station 3 and Station 6 are presented in panel A. The seawater transects in the South Atlantic Ocean: Antarctic Intermediate Water (AAIW), Upper Circumpolar Deep Water (UCDW), North Atlantic Deep Water (NADW), and Antarctic Bottom Water (AABW). Panel B shows the seawater $\delta^{51}V$ zoom-in of the euphotic zone (< 100 m) at Station 3 and Station 6. Panel C shows the $\delta^{51}V$ values of two seawater samples collected in the Black Sea. The gray bar indicates the seawater $\delta^{51}V$ values in open oceans measured by Wu et al. (2019). The error bars are long-term in-lab 2SD of BDH-V standard solutions, unless the sample uncertainty is worse than that. A 2SD value of 0.16 ‰ is assigned to the Black Sea seawater samples based on the worst data uncertainty of our isotope measurement.

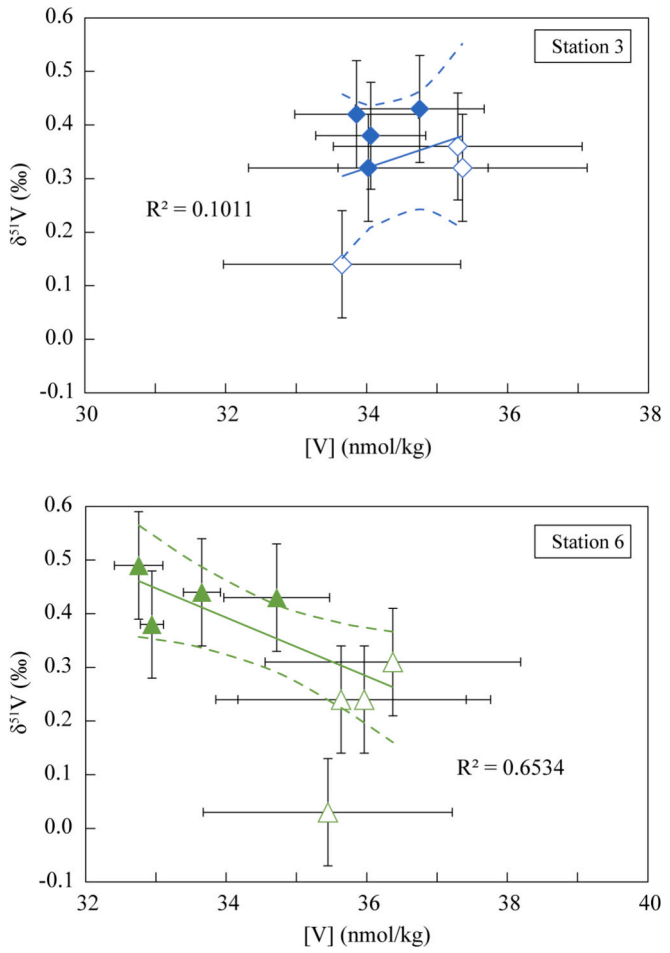

Fig. 7. The simple linear regression (solid line) and 95 % confidence interval of the regression (dashed lines) for seawater V concentrations ([V]) and isotopic compositions ($\delta^{51}V$) at Station 3 (blue diamonds) and Station 6 (green triangles). The filled symbols are shallow seawater samples (<100 m) within the euphotic zone and the open symbols are deep seawater samples (>100 m). For Station 6, the AABW sample is eliminated from the regression analysis due to potential regional influence (see *Discussion*).

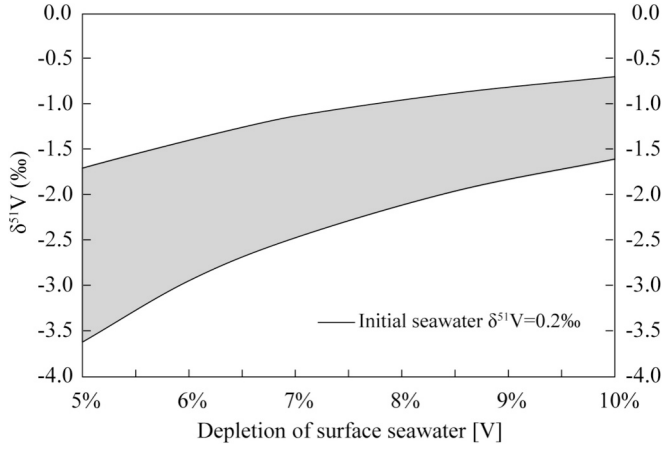

Fig. 8. The potential $\delta^{51}V$ signatures carried by the biota in the euphotic zone as indicated by the gray area during the biological uptake of V, resulting in a positive shifting of the surface seawater $\delta^{51}V$ values by 0.1 ‰ (the upper boundaries) to 0.2 ‰ (the lower boundaries).

investigated the $\delta^{51}V$ signatures in one zooplankton sample and two benthic algae samples from a lake system, which are approximately 0.2 ‰ lower than the $\delta^{51}V$ values of the lake sediments. Although the $\delta^{51}V$ values of the lake water were not measured——preventing calculation of the isotopic fractionation factor associated with biological uptake——this work nonetheless suggests a preferential uptake of ^{50}V during biological processes. This is inferred from the preferential burial of ^{50}V in sediments, which would leave the water relatively enriched in ^{51}V (Nielsen, 2020 and reference therein). However, whether V has a specific biological function in marine phytoplankton is currently unknown, since the few biological processes in which V takes part are not unambiguously associated with marine phytoplankton (Bellenger et al., 2008; Winter and Moore, 2009).

The AABW shows a relatively lower $\delta^{51}V$ value of 0.03 ‰ than in overlying water masses. This greater deviation from other deep seawater $\delta^{51}V$ values may indicate some local/regional processes that happen during the formation and/or transportation of AABW—for instance, the influence relevant to the continental weathering and acidic rock drainage from Antarctica continent (Dold et al., 2013; Siqueira et al., 2021). The weathering influence may deviate seawater $\delta^{51}V$ value owing to inputs of lower V isotopic compositions that are similar to the bedrock (Qi et al., 2022; Schuth et al., 2019).

5.2. *The Black Sea surface seawater [V] and $\delta^{51}V$ signatures*

The two seawater samples collected from the Black Sea at depths of 100 and 150 m contain similar V concentrations at 16.1 and 15.2 nmol/kg (Table 2 and Fig. 5C). In contrast to the seawater $\delta^{51}V$ signatures in open oceans, the two seawater samples from the Black Sea demonstrate lower $\delta^{51}V$ values at 0.17 and −0.07 ‰ (Table 2 and Fig. 6C). The relatively low salinity in the Black Sea indicates that there is an influence from local riverine inputs, as rainfall makes limited contributions to seawater V, and the rainfall flux is roughly equal to the evaporation flux in the Black Sea Basin (Kara et al., 2008). However, the conservative mixing of riverine runoffs and seawater, as estimated based on the Black Sea seawater salinity between 18 and 22 psu from the surface across the chemocline (Vance et al., 2016), shows deviations from observed Black Sea seawater [V] and $\delta^{51}V$ values (Fig. 9). Previous research indicates lateral Mn and Fe transport from coastal sediments to the water column chemocline in the Black Sea (Yemenicioglu et al., 2006; Lenstra et al., 2019, 2020) which may contribute lower $\delta^{51}V$ fluxes to the redox chemocline zone (Chen et al., 2022), superimposed on the seawater column [V] and $\delta^{51}V$ values based on the conservative seawater–river water mixing processes (Fig. 9). Addition of Mn and Fe oxides to the chemocline zone would lower the $\delta^{51}V$ values, but concomitantly increase the water column [V] further from the conservative mixing relationship (Fig. 9). On the other hand, as ^{50}V is preferentially removed from water columns and buried in Black Sea sediments (Chen et al., 2022), this should leave the seawater with lower [V] values (Emerson and Huested, 1991) along with heavier deep water $\delta^{51}V$ signatures. Thus, it is possible that the basinal vertical circulation as constrained by previous research (Stanev et al., 2002; Stanev, 2005) can lower the seawater V concentrations and simultaneously buffer the lighter seawater $\delta^{51}V$ values resulting from riverine inputs and/or oxide shuttle (Fig. 9). However, it is difficult to quantify such processes due to unknown deep water $\delta^{51}V$ signatures in the Black Sea and the poor constraints over the V fluxes and $\delta^{51}V$ signatures from surrounding riverine runoffs and/or basinal Fe–Mn oxide shuttling. The seawater Mo isotopic signatures in the Black Sea also suggest such vertical mixing processes (Nägler et al., 2011). It is important to note that the above processes are discussed to reflect underlying processes responsible for observed seawater [V] and $\delta^{51}V$ values across the anoxic-to-euxinic boundary in the shallow water column but not to indicate the basin-scale V mass budget in the Black Sea. Instead, the preliminary evaluation of the V mass budget considering riverine inputs, sedimentary burial, and Bosporus inflows and outflows likely indicates an unbalanced state, although large uncertainties

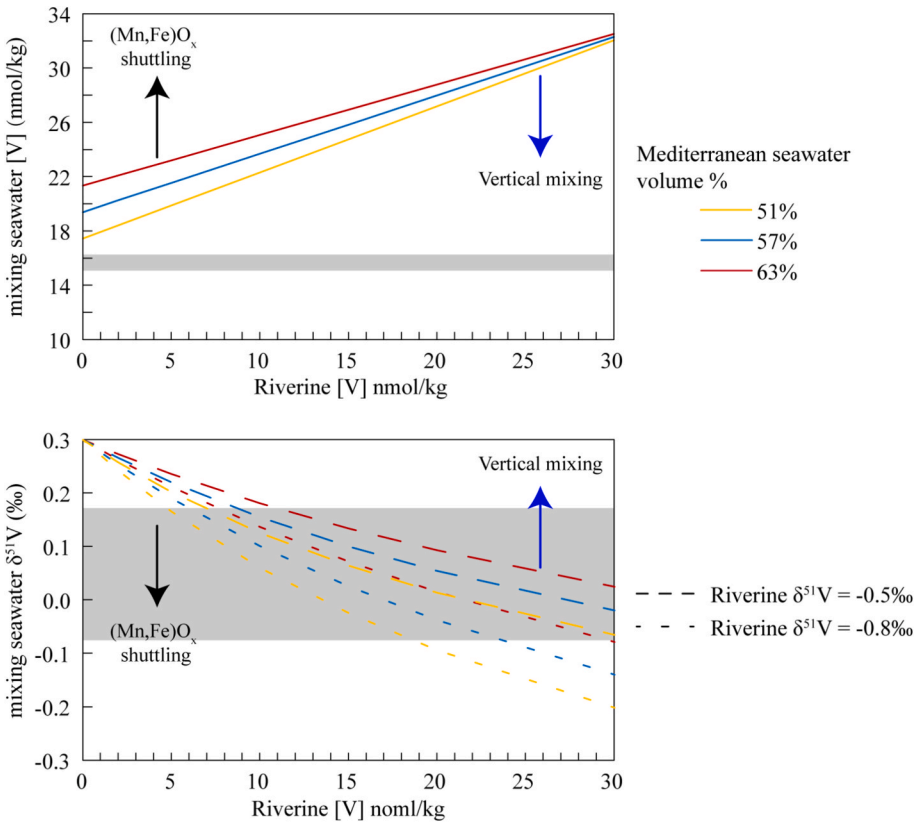

Fig. 9. The Black Sea seawater [V] (upper pane) and $\delta^{51}V$ values (lower panel) in shallow layers as estimated with the conservative Mediterranean seawater–river mixing model. The Black Sea seawater salinity range (S = 18–22 ‰) is used as the boundary condition to constrain the possible mixing volume ratios of the Mediterranean seawater (salinity S = 35 ‰) through Bosporus Strait and riverine runoffs (S = 0). The volume contributions of the Mediterranean seawater thus are 51, 57, and 63 % as calculated based on Black Sea seawater salinity values at 18, 20, and 22, respectively. Mediterranean seawater [V] and $\delta^{51}V$ values are set as 34 nmol/kg (Sherrell and Boyle, 1988) and 0.3 ‰, respectively. The riverine [V] range is referred to Shiller and Mao (2000) and the sensitivity tests on riverine $\delta^{51}V$ values are set referring to Schuth et al. (2019) and Wu et al. (2019). The shaded bar in the upper panel shows the observed Black Sea seawater [V] values. The shaded area in the lower panel indicates the Black Sea seawater $\delta^{51}V$ values –0.07 and 0.17 ‰. The influence of lateral Mn and Fe oxide shuttling, imposed on the conservative seawater–river mixing, is illustrated with the black arrow. The blue arrow indicates the influence of the basinal vertical mixing processes.

remain due to absent constraints on certain critical parameters and wide ranges of investigated parameters (see *Appendix A. Supplementary Material*).

Moreover, based on the seawater $\delta^{51}V$ values across the anoxic-to-euxinic boundary, the apparent V isotopic offsets between the seawater and the authigenic euxinic sedimentary V in the Black Sea would be around 0.4 to 0.7 ‰ (Chen et al., 2022), as V is proposed to be removed near the bottom of the chemocline zone by sinking particulates (Wu et al., 2020). The apparent isotopic offsets in the Black Sea are similar to the range documented in the anoxic but non-euxinic conditions in the open marine settings and the euxinic sediments in the Cariaco Basin (Wu et al., 2020). The salinity of Cariaco seawater is around 36–37 psu (McConnell et al., 2009); thus we presume that the shallow seawater $\delta^{51}V$ values above the bottom of the chemocline in the Cariaco Basin are similar to the Atlantic Ocean. This indicates limited isotope fractionations correlated to H_2S, despite wide variations in the water column [H_2S] from 0 under non-euxinic conditions to around 30–40 μmol/L in the deep water column in the Cariaco Basin (Taylor et al., 2001) and > 300 μmol/L in the deep Black Sea (Neretin et al., 2001). Therefore, the isotopic fractionation under steady state is likely achieved as V is removed near the bottom of the chemocline zone, which seems not to be closely correlated with H_2S. This is also suggested by relatively constant seawater [V] values in deep euxinic water columns despite increasing [H_2S] (Emerson and Huested, 1991) and consistent sedimentary authigenic $\delta^{51}V$ values under euxinic conditions at different depths (at ~ 200 m and > 2000 m) in the Black Sea (Chen et al., 2022). Collectively, these observations support previous conclusions in which V deposition in low-oxygen sediments is controlled primarily by uptake into organic matter rather than related to sulfide precipitation (Nielsen, 2020). Nonetheless, the limited data points encourage future investigation of the seawater $\delta^{51}V$ profiles in euxinic basins to better understand V isotope cycling in euxinic environments.

5.3. *Implications of utilizing vanadium isotopes to constrain ancient marine redox conditions*

Vanadium is mainly scavenged from the seawater by sinking particulates (e.g., Mn and Fe oxides and organic particulates) with corresponding isotope fractionations that characterize different redox (oxic, anoxic, and euxinic) environments (Nielsen, 2020 and reference therein). Previous research (Li et al., 2023) shows that this proxy can be utilized to track the low-oxygen-to-anoxic fluctuations in the bottom water, which are not identified by other redox proxies (e.g., Fe speciation). The primary influence from local depositional conditions is further testified to by the global homogeneity of seawater V isotopic signatures in deep seawater masses. Correspondingly, the sedimentary $\delta^{51}V$ profile under the relatively well-constrained local redox conditions through a multi-proxy method can also reflect the first-order control from the variations of the seawater $\delta^{51}V$ signature in response to marine redox perturbations at global or basinal scales (Heard et al., 2023; Li et al., 2023; Wei et al., 2023), albeit potential post-depositional alterations also need to be considered in future work on V isotopes. Caution should also be taken in the interpretation of ancient marine sedimentary archives in cases of shallow marine environments (i.e., potential

biological influence within the euphotic zone) and restricted epicontinental basins (this study; Chen et al., 2022). Additionally, interpreting restricted conditions with V isotopes could be paired with additional geochemical redox proxies (e.g., Mo/U ratio, Algeo and Tribovillard, 2009; Tl isotopes, Owens et al., 2017).

6. Conclusions

We studied the seawater $\delta^{51}V$ profiles intersecting major global water masses at ~ 40°S in the South Atlantic Ocean and the $\delta^{51}V$ values of two seawater samples collected from the shallow water columns across the anoxic-to-euxinic chemocline in the Black Sea, aiming to explore the potential influences on the seawater $\delta^{51}V$ values from large-scale ocean circulations and local/regional hydrological and biogeochemical processes. This dataset has also increased available seawater data for the open oceans from only six samples (Wu et al., 2019) to 22 samples, which now cover the major ocean water masses that participate in open ocean circulations. However, as this work has shown, there could be small-scale variations in local environments that are not observed in this dataset.

The results robustly confirm the relatively homogeneous seawater $\delta^{51}V$ signatures in deep open oceans. The values of deep seawater masses (>100 m) that are sourced from different locations present an average of 0.27 ‰ ± 0.14 ‰ (2SD, excluding the Antarctic bottom water sample owing to the potential influence from Antarctica weathering input). This is consistent with the previously reported average seawater $\delta^{51}V$ value at 0.20 ‰ ± 0.15 ‰ (2SD) in open oceans (Wu et al., 2019). However, the local impacts, such as the biological uptake in the euphotic zone and the riverine inputs to the near-coast environments or severely restricted basins, may alter the seawater $\delta^{51}V$ signals, implying that ancient marine sedimentary $\delta^{51}V$ records preserved under similar conditions should be interpreted carefully.

The $\delta^{51}V$ values of the two seawater samples collected from the shallow water columns across the anoxic-to-euxinic chemocline in the Black Sea are at 0.17 and −0.07 ‰. The underlying processes regulating seawater [V] and $\delta^{51}V$ likely include local hydrological mixing processes and biogeochemical V cycling, such as the seawater–river blending, the lateral coast-to-deep basin Fe and Mn oxide shuttling, and the basinal vertical mixing processes. Based on the observed albeit very limited seawater $\delta^{51}V$ values, the isotopic offsets between seawater and euxinic sediments in the Black Sea are similar to the values documented in the anoxic and non-euxinic conditions in the open oceans and the euxinic sediments in the Cariaco Basin, despite large variations in aqueous chemistry (e.g., $[H_2S]$ in water columns). Future work investigating the seawater $\delta^{51}V$ profiles in euxinic basins can promote the fundamental understanding of V isotope cycling in euxinic environments.

CRediT authorship contribution statement

Siqi Li: Writing – review & editing, Writing – original draft, Visualization, Methodology, Investigation, Formal analysis. **Sune G. Nielsen:** Writing – review & editing, Resources, Funding acquisition. **Jeremy D. Owens:** Writing – review & editing, Supervision, Funding acquisition, Conceptualization.

Declaration of competing interest

The authors declare that they have no known competing financial interests or personal relationships that could have appeared to influence the work reported in this paper.

Acknowledgements

We thank G. White for instrumentation troubleshooting at the National High Magnetic Field Laboratory. We acknowledge support from the NSF-OCE 1434785/1624895 (to J.D.O. and S.G.N.) and the NASA Exobiology Grant NNX16AJ60G (to J.D.O. and S.G.N). JDO would like to thank the Sloan Foundation (FG-2020–13552). This work was performed at the National High Magnetic Field Laboratory in Tallahassee, Florida, which is supported by National Science Foundation Cooperative Agreement DMR-1644779 and by the State of Florida.

Appendix A. Supplementary material

The supplementary material provides the estimates of the V mass budget in the Black Sea. Supplementary material to this article can be found online at https://doi.org/10.1016/j.gca.2025.08.037.

Data availability

Data are available through BCO-DMO at https://www.bco-dmo.org/dataset/957165.

References

Algeo, T.J., Tribovillard, N., 2009. Environmental analysis of paleoceanographic systems based on molybdenum–uranium covariation. Chem. Geol. 268, 211–225.
Andersson, I., Angus-Dunne, S., Howarth, O., Pettersson, L., 2000. Speciation in vanadium bioinorganic systems: 6. Speciation study of aqueous peroxovanadates, including complexes with imidazole. J. Inorg. Biochem. 80, 51–58.
Archer, C., Vance, D., Milne, A., Lohan, M.C., 2020. The oceanic biogeochemistry of nickel and its isotopes: New data from the South Atlantic and the Southern Ocean biogeochemical divide. Earth Planet. Sci. Lett. 535, 116118.
Arthur, M.A., Dean, W.E., 1998. Organic-matter production and preservation and evolution of anoxia in the Holocene Black Sea. Paleoceanography 13, 395–411.
Bellenger, J.P., Wichard, T., Kustka, A.B., Kraepiel, A.M.L., 2008. Uptake of molybdenum and vanadium by a nitrogen-fixing soil bacterium using siderophores. Nat. Geosci. 1, 243–246.
Berner, R.A., 2013. An earth systems diagram for the global cycles of carbon and phosphorus and their effects on atmospheric CO2 and O2. Aquat. Geochem. 19, 565–568.
Chen, X., Li, S., Newby, S.M., Lyons, T.W., Wu, F., Owens, J.D., 2022. Iron and manganese shuttle has no effect on sedimentary thallium and vanadium isotope signatures in Black Sea sediments. Geochim. Cosmochim. Acta 317, 218–233.
Chételat, J., Nielsen, S.G., Auro, M., Carpenter, D., Mundy, L., Thomas, P.J., 2021. Vanadium stable isotopes in biota of terrestrial and aquatic food chains. Environ. Sci. Technol. 55, 4813–4821.
Cole, D.B., Mills, D.B., Erwin, D.H., Sperling, E.A., Porter, S.M., Reinhard, C.T., Planavsky, N.J., 2020. On the co-evolution of surface oxygen levels and animals. Geobiology 18, 260–281.
Collier, R.W., 1984. Particulate and dissolved vanadium in the North Pacific Ocean. Nature 309, 441.
Conway, T.M., John, S.G., Lacan, F., 2016. Intercomparison of dissolved iron isotope profiles from reoccupation of three GEOTRACES stations in the Atlantic Ocean. Mar. Chem. 183, 50–61.
Dold, B., Gonzalez-Toril, E., Aguilera, A., Lopez-Pamo, E., Cisternas, M.E., Bucchi, F., Amils, R., 2013. Acid rock drainage and rock weathering in antarctica: important sources for iron cycling in the Southern Ocean. Environ. Sci. Technol. 47, 6129–6136.
Eckert, S., Brumsack, H.-J., Severmann, S., Schnetger, B., März, C., Fröllje, H., 2013. Establishment of euxinic conditions in the Holocene Black Sea. Geology 41, 431–434.
Emerson, S.R., Huested, S.S., 1991. Ocean anoxia and the concentrations of molybdenum and vanadium in seawater. Mar. Chem. 34, 177–196.
Evans, S.D., Diamond, C.W., Droser, M.L., Lyons, T.W., 2018. Dynamic oxygen and coupled biological and ecological innovation during the second wave of the Ediacara Biota. Emerg. Top. Life Sci. 2, 223–233.
GA04N Section (leg 2) – Cruise 64PE373; Mediterranean and Black Sea, Lisbon (Portugal) to Istanbul (Turkey) – GEOTRACES [WWW Document], n.d.
Gordon, A.L., 2001. Bottom water formation. Elsevier. In: Encyclopedia of Ocean Sciences, pp. 334–340.
Heard, A.W., Wang, Y., Ostrander, C.M., Auro, M., Canfield, D.E., Zhang, S., Wang, H., Wang, X., Nielsen, S.G., 2023. Coupled vanadium and thallium isotope constraints on Mesoproterozoic ocean oxygenation around 1.38-1.39 Ga. Earth Planet. Sci. Lett. 610, 118127.
Ho, P., Lee, J.-M., Heller, M.I., Lam, P.J., Shiller, A.M., 2018. The distribution of dissolved and particulate Mo and V along the U.S. GEOTRACES East Pacific Zonal Transect (GP16): The roles of oxides and biogenic particles in their distributions in the oxygen deficient zone and the hydrothermal plume. Mar. Chem., The U.S. GEOTRACES Eastern Tropical Pacific Transect (GP16) 201, 242–255.
Horner, T.J., Kinsley, C.W., Nielsen, S.G., 2015. Barium-isotopic fractionation in seawater mediated by barite cycling and oceanic circulation. Earth Planet. Sci. Lett. 430, 511–522.
Kara, A.B., Wallcraft, A.J., Hurlburt, H.E., Stanev, E.V., 2008. Air–sea fluxes and river discharges in the Black Sea with a focus on the Danube and Bosphorus. J. Mar. Syst. 74, 74–95.

Kendall, B., Dahl, T.W., Anbar, A.D., 2017. The stable isotope geochemistry of molybdenum. Rev. Mineral. Geochem. 82, 683–732.

Lenstra, W.K., Hermans, M., Séguret, M.J.M., Witbaard, R., Behrends, T., Dijkstra, N., van Helmond, N.A.G.M., Kraal, P., Laan, P., Rijkenberg, M.J.A., Severmann, S., Teacă, A., Slomp, C.P., 2019. The shelf-to-basin iron shuttle in the Black Sea revisited. Chem. Geol. 511, 314–341.

Lenstra, W.K., Séguret, M.J.M., Behrends, T., Groeneveld, R.K., Hermans, M., Witbaard, R., Slomp, C.P., 2020. Controls on the shuttling of manganese over the northwestern Black Sea shelf and its fate in the euxinic deep basin. Geochim. Cosmochim. Acta 273, 177–204.

Li, S., Friedrich, O., Nielsen, S.G., Wu, F., Owens, J.D., 2023. Reconciling biogeochemical redox proxies: Tracking variable bottom water oxygenation during OAE-2 using vanadium isotopes. Earth Planet. Sci. Lett. 617, 118237.

Lindskog, A., Young, S.A., Bowman, C.N., Kozik, N.P., Newby, S.M., Eriksson, M.E., Pettersson, J., Molin, E., Owens, J.D., 2023. Oxygenation of the Baltoscandian shelf linked to Ordovician biodiversification. Nat. Geosci. 16, 1047–1053.

Lutjeharms, J.R.E. (Ed.), 2006. The Agulhas Current retroflection, in: The Agulhas Current. Springer, Berlin, Heidelberg, pp. 151–207.

Lyons, T.W., Reinhard, C.T., Planavsky, N.J., 2014. The rise of oxygen in Earth's early ocean and atmosphere. Nature 506, 307–315.

Mawji, E., Schlitzer, R., Dodas, E.M., Abadie, C., Abouchami, W., Anderson, R.F., Baars, O., Bakker, K., Baskaran, M., Bates, N.R., Bluhm, K., Bowie, A., Bown, J., Boye, M., Boyle, E.A., Branellec, P., Bruland, K.W., Brzezinski, M.A., Bucciarelli, E., Buesseler, K., Butler, E., Cai, P., Cardinal, D., Casciotti, K., Chaves, J., Cheng, H., Chever, F., Church, T.M., Colman, A.S., Conway, T.M., Croot, P.L., Cutter, G.A., de Baar, H.J.W., de Souza, G.F., Dehairs, F., Deng, F., Dieu, H.T., Dulaquais, G., Echegoyen-Sanz, Y., Lawrence Edwards, R., Fahrbach, E., Fitzsimmons, J., Fleisher, M., Frank, M., Friedrich, J., Fripiat, F., Galer, S.J.G., Gamo, T., Solsona, E. G., Gerringa, L.J.A., Godoy, J.M., Gonzalez, S., Grossteffan, E., Hatta, M., Hayes, C. T., Heller, M.I., Henderson, G., Huang, K.-F., Jeandel, C., Jenkins, W.J., John, S., Kenna, T.C., Klunder, M., Kretschmer, S., Kumamoto, Y., Laan, P., Labatut, M., Lacan, F., Lam, P.J., Lannuzel, D., le Moigne, F., Lechtenfeld, O.J., Lohan, M.C., Lu, Y., Masqué, P., McClain, C.R., Measures, C., Middag, R., Moffett, J., Navidad, A., Nishioka, J., Noble, A., Obata, H., Ohnemus, D.C., Owens, S., Planchon, F., Pradoux, C., Puigcorbé, V., Quay, P., Radic, A., Rehkämper, M., Remenyi, T., Rijkenberg, M.J.A., Rintoul, S., Robinson, L.F., Roeske, T., Rosenberg, M., van der Loeff, M.R., Ryabenko, E., Saito, M.A., Roshan, S., Salt, L., Sarthou, G., Schauer, U., Scott, P., Sedwick, P.N., Sha, L., Shiller, A.M., Sigman, D.M., Smethie, W., Smith, G. J., Sohrin, Y., Speich, S., Stichel, T., Stutsman, J., Swift, J.H., Tagliabue, A., Thomas, A., Tsunogai, U., Twining, B.S., van Aken, H.M., van Heuven, S., van Ooijen, J., van Weerlee, E., Venchiarutti, C., Voelker, A.H.L., Wake, B., Warner, M.J., Woodward, E.M.S., Wu, J., Wyatt, N., Yoshikawa, H., Zheng, X.-Y., Xue, Z., Zieringer, M., Zimmer, L.A., 2015. The GEOTRACES Intermediate Data Product 2014. Mar. Chem. Biogeochemistry of Trace Elements and their Isotopes 177, 1–8.

McConnell, M.C., Thunell, R.C., Lorenzoni, L., Astor, Y., Wright, J.D., Fairbanks, R., 2009. Seasonal variability in the salinity and oxygen isotopic composition of seawater from the Cariaco Basin, Venezuela: Implications for paleosalinity reconstructions. Geochem. Geophys. Geosyst. 10.

Mlddelburg, J.J., Hoede, D., Van Der Sloot, H.A., Van Der Weijden, C.H., Wijkstra, J., 1988. Arsenic, antimony and vanadium in the North Atlantic Ocean. Geochim. Cosmochim. Acta 52, 2871–2878.

Moore, E.K., Jelen, B.I., Giovannelli, D., Raanan, H., Falkowski, P.G., 2017. Metal availability and the expanding network of microbial metabolisms in the Archaean eon. Nat. Geosci. 10, 629–636.

Nägler, T.F., Neubert, N., Böttcher, M.E., Dellwig, O., Schnetger, B., 2011. Molybdenum isotope fractionation in pelagic euxinia: evidence from the modern Black and Baltic Seas. Chem. Geol. 289, 1–11.

Neretin, L.N., Volkov, I.I., Böttcher, M.E., Grinenko, V.A., 2001. A sulfur budget for the Black Sea anoxic zone. Deep Sea Res. Part Oceanogr. Res. Pap. 48, 2569–2593.

Nielsen, S.G., 2020. Vanadium Isotopes: a proxy for ocean oxygen variations. Elem. Geochem. Tracers Earth Syst. Sci.

Nielsen, S.G., Owens, J.D., Horner, T.J., 2016. Analysis of high-precision vanadium isotope ratios by medium resolution MC-ICP-MS. J. Anal. At. Spectrom 31, 531–536.

Nielsen, S.G., Prytulak, J., Halliday, A.N., 2011. Determination of Precise and Accurate 51V/50V Isotope Ratios by MC-ICP-MS, Part 1: Chemical Separation of Vanadium and Mass Spectrometric Protocols. Geostand. Geoanalytical Res. 35, 293–306.

Owens, J.D., Nielsen, S.G., Horner, T.J., Ostrander, C.M., Peterson, L.C., 2017. Thallium-isotopic compositions of euxinic sediments as a proxy for global manganese-oxide burial. Geochim. Cosmochim. Acta 213, 291–307.

Owens, J.D., Reinhard, C.T., Rohrssen, M., Love, G.D., Lyons, T.W., 2016. Empirical links between trace metal cycling and marine microbial ecology during a large perturbation to Earth's carbon cycle. Earth Planet. Sci. Lett. 449, 407–417.

Paul, M., van de Flierdt, T., Rehkämper, M., Khondoker, R., Weiss, D., Lohan, M.C., Homoky, W.B., 2015. Tracing the Agulhas leakage with lead isotopes. Geophys. Res. Lett. 42, 8515–8521.

Qi, Y.-H., Gong, Y.-Z., Wu, F., Lu, Y., Cheng, W., Huang, F., Yu, H.-M., 2022. Coupled variations in V-Fe abundances and isotope compositions in latosols: Implications for V mobilization during chemical weathering. Geochim. Cosmochim. Acta 320, 26–40.

Reinhard, C.T., Planavsky, N.J., Ward, B.A., Love, G.D., Le Hir, G., Ridgwell, A., 2020. The impact of marine nutrient abundance on early eukaryotic ecosystems. Geobiology 18, 139–151.

Robbins, L.J., Lalonde, S.V., Planavsky, N.J., Partin, C.A., Reinhard, C.T., Kendall, B., Scott, C., Hardisty, D.S., Gill, B.C., Alessi, D.S., Dupont, C.L., Saito, M.A., Crowe, S. A., Poulton, S.W., Bekker, A., Lyons, T.W., Konhauser, K.O., 2016. Trace elements at the intersection of marine biological and geochemical evolution. Earth Sci. Rev. 163, 323–348.

Schuth, S., Brüske, A., Hohl, S.V., Jiang, S.-Y., Meinhardt, A.-K., Gregory, D.D., Viehmann, S., Weyer, S., 2019. Vanadium and its isotope composition of river water and seawater: Analytical improvement and implications for vanadium isotope fractionation. Chem. Geol.

Sherrell, R.M., Boyle, E.A., 1988. Zinc, chromium, vanadium and iron in the Mediterranean Sea. Deep Sea Res. Part Oceanogr. Res. Pap. 35, 1319–1334.

Shiller, A.M., Mao, L., 2000. Dissolved vanadium in rivers: effects of silicate weathering. Chem. Geol. 165, 13–22.

Siqueira, R.G., Schaefer, C.E.G.R., Fernandes Filho, E.I., Corrêa, G.R., Francelino, M.R., de Souza, J.J.L.L., Rocha, P. de A., 2021. Weathering and pedogenesis of sediments and basaltic rocks on Vega Island, Antarctic Peninsula. Geoderma 382, 114707.

Solodoch, A., Stewart, A.L., Hogg, A.M., Morrison, A.K., Kiss, A.E., Thompson, A.F., Purkey, S.G., Cimoli, L., 2022. How does antarctic bottom water cross the southern ocean? Geophys. Res. Lett. 49, e2021GL097211.

Sperling, E.A., Boag, T.H., Duncan, M.I., Endriga, C.R., Marquez, J.A., Mills, D.B., Monarrez, P.M., Sclafani, J.A., Stockey, R.G., Payne, J.L., 2022. Breathless through time: oxygen and animals across earth's history. Biol. Bull. 243, 184–206.

Stanev, E., 2005. Understanding black sea dynamics: overview of recent numerical modeling. Oceanography 18, 56–75.

Stanev, E.V., Beckers, J.M., Lancelot, C., Staneva, J.V., Le Traon, P.Y., Peneva, E.L., Gregoire, M., 2002. Coastal–open ocean exchange in the black sea: observations and modelling. Estuar. Coast. Shelf Sci. 54, 601–620.

Stanev, E.V., Simeonov, J.A., Peneva, E.L., 2001. Ventilation of Black Sea pycnocline by the Mediterranean plume. J. Mar. Syst., Ventilation of Black Sea Anoxic Waters 31, 77–97.

Taylor, G.T., Iabichella, M., Ho, T.-Y., Scranton, M.I., Thunell, R.C., Muller-Karger, F., Varela, R., 2001. Chemoautotrophy in the redox transition zone of the Cariaco Basin: a significant midwater source of organic carbon production. Limnol. Oceanogr. 46, 148–163.

Vance, D., Little, S.H., Archer, C., Cameron, V., Andersen, M.B., Rijkenberg, M.J.A., Lyons, T.W., 2016. The oceanic budgets of nickel and zinc isotopes: the importance of sulfidic environments as illustrated by the Black Sea. Philos. Trans. R. Soc. Math. Phys. Eng. Sci. 374, 20150294.

Wei, W., Chen, X., Ling, H.-F., Wu, F., Dong, L.-H., Pan, S., Jing, Z., Huang, F., 2023. Vanadium isotope evidence for widespread marine oxygenation from the late Ediacaran to early Cambrian. Earth Planet. Sci. Lett. 602, 117942.

Winter, J.M., Moore, B.S., 2009. Exploring the chemistry and biology of vanadium-dependent haloperoxidases. J. Biol. Chem. 284, 18577–18581.

Wu, F., Owens, J.D., Huang, T., Sarafian, A., Huang, K.-F., Sen, I.S., Horner, T.J., Blusztajn, J., Morton, P., Nielsen, S.G., 2019. Vanadium isotope composition of seawater. Geochim. Cosmochim. Acta 244, 403–415.

Wu, F., Owens, J.D., Scholz, F., Huang, L., Li, S., Riedinger, N., Peterson, L.C., German, C. R., Nielsen, S.G., 2020. Sedimentary vanadium isotope signatures in low oxygen marine conditions. Geochim. Cosmochim. Acta 284, 134–155.

Wu, F., Qi, Y., Yu, H., Tian, S., Hou, Z., Huang, F., 2016. Vanadium isotope measurement by MC-ICP-MS. Chem. Geol. 421, 17–25.

Wyatt, N.J., Milne, A., Woodward, E.M.S., Rees, A.P., Browning, T.J., Bouman, H.A., Worsfold, P.J., Lohan, M.C., 2014. Biogeochemical cycling of dissolved zinc along the GEOTRACES South Atlantic transect GA10 at 40°S. Glob. Biogeochem. Cycles 28, 44–56.

Yemenicioglu, S., Erdogan, S., Tugrul, S., 2006. Distribution of dissolved forms of iron and manganese in the Black Sea. Deep Sea Res. Part II Top. Stud. Oceanogr Black Sea Oceanography 53, 1842–1855.

Zhang, F., Lenton, T.M., del Rey, Á., Romaniello, S.J., Chen, X., Planavsky, N.J., Clarkson, M.O., Dahl, T.W., Lau, K.V., Wang, W., Li, Z., Zhao, M., Isson, T., Algeo, T. J., Anbar, A.D., 2020. Uranium isotopes in marine carbonates as a global ocean paleoredox proxy: A critical review. Geochim. Cosmochim. Acta, New developments in geochemical proxies for paleoceanographic research 287, 27–49.